



Research paper

Singularities of ABB's YuMi 7-DOF robot arm

Milad Asgari^a, Ilian A. Bonev^{a, ID, *}, Clément Gosselin^{b, ID}^a École de technologie supérieure (ÉTS), Montreal, QC, Canada^b Université Laval, Quebec City, QC, Canada

ARTICLE INFO

Keywords:

Singular configurations

Singularity analysis

Redundant manipulator

YuMi

ABSTRACT

ABB's YuMi is a unique, innovative cobot but it is also one of the most challenging 7-degree-of-freedom (DOF) robot arms on the market, in terms of kinematics. Indeed, unlike some other 7-DOF robot arms with revolute joints, in YuMi, consecutive joint axes are normal to each other, but not intersecting. And despite being invented over a decade ago, there is surprisingly little information available about its kinematics. To effectively incorporate this manipulator into motion planning tasks, it is essential to have a comprehensive grasp of its arm angle and singularities. In this paper, we use the screw dependency approach with a novel combinatorial technique and Grassmann geometry of lines to identify and categorize, for the first time, the kinematic singularities of YuMi based on simple geometrical conditions. This methodology allows for a systematic and clear understanding of the robot's singular configurations. In addition, we provide the definition of the arm angle used by ABB and a formula for the angle calculation. Then, we describe the representation singularity, and explain the algorithmic singularities that are related to the arm angle.

1. Introduction

Seven-degree-of-freedom (7-DOF) manipulators present greater design and operational challenges compared to 6-DOF arms due to the additional DOF, which complicates inverse kinematics and singularities. However, 7-DOF manipulators offer significant advantages in some applications. The extra DOF enhances the robot's agility, enabling it to avoid obstacles and singularities and improve overall manipulability [1,2]. Redundant manipulators used to be reserved mainly for spatial and research applications [3]. Today, there are many examples of 7-DOF industrial robots, such as FANUC's R-1000iA/120F-7B, KUKA's iiwa, and the cobots of Kasso Robots, Franka Robotics and Productive Robotics, as well as ABB's YuMi.

A few 7-DOF robot arms (e.g., KUKA's iiwa and Yaskawa's SIA series) have a simple 7R (7-revolute-joint) kinematic structure from a geometrical point of view, where the joint axes in each of the following three groups are concurrent: {1,2,3} (shoulder), {3,4,5} (elbow), and {5,6,7} (wrist), and every two consecutive axes are normal to each other. In the other popular 7R architecture, assumed by most space manipulators (e.g., the Canadarm2), the middle three joint axes are parallel.

A simple 7-DOF kinematic architecture loosely means that singularities are easy to describe (and therefore deal with), and the inverse kinematics have an analytical solution. A 6R arm, for example, is considered to have a complex structure if it lacks any combination of three parallel axes or three axes intersecting at a single point [4]. Of course, an analytical solution is always preferable to a numerical method because it works flawlessly and provides a simple method for specifying the desired solution through so-called *configuration parameters* (typically Boolean variables determining which of two solutions for certain joint angles

* Corresponding author.

E-mail address: ilian.bonev@etsmtl.ca (I.A. Bonev).<https://doi.org/10.1016/j.mechmachtheory.2024.105884>

Received 23 June 2024; Received in revised form 3 December 2024; Accepted 4 December 2024

Available online 17 December 2024

0094-114X/© 2024 The Authors.

Published by Elsevier Ltd.

This is an open access article under the CC BY license

<http://creativecommons.org/licenses/by/4.0/>.

is selected) and—in the case of 7R arms—the *arm angle*, which is the variable associated with the redundant DOF, also called a *self motion* [5].

In the more recent, single-arm version of ABB's YuMi, IRB 14050, which is the same as each of the two arms of the original YuMi, IRB 14000, no two axes are permanently parallel or intersecting at a constant point, and a numerical method is used for solving the robot's inverse kinematics. YuMi has the same kinematic structure as the robot arm studied in [5]. The joint offsets in YuMi enable a larger workspace and improved reachability compared to a 7R robot arm without joint offsets such as KUKA's iiwa. For the same reasons, many manufacturers of 7R and 6R cobots have adopted designs with joint offsets (e.g., Kassow Robots, Productive Robotics, Fanuc and Kinova).

Every 7-DOF cobot brand likely manages singularities, the self-motion variable, and inverse kinematics parameters differently. In the case of ABB's YuMi, which this paper specifically addresses, not understanding these three kinematic elements can make programming cumbersome, despite the clear advantages of hand-guiding. Hence, it is crucial to conduct an analysis of the inverse kinematics and singularities of this manipulator and provide a clear definition for the arm angle.

In 7-DOF robot arms, there are two types of singular configurations: *kinematic singularities* and *algorithmic singularities* [5]. A kinematic singularity is a configuration where the robot end-effector loses the ability to move in at least one direction [6]. When a manipulator is in a kinematic singularity, the Jacobian matrix becomes rank-deficient. For a 6-DOF manipulator, since the Jacobian is a 6×6 matrix, singularities occur when $\det(\mathbf{J}) = 0$ [7]. However, for a 7-DOF redundant manipulator like YuMi, the Jacobian is a 6×7 matrix and does not have a determinant to analyze the singularities. Therefore, some researchers have utilized Whitney's approach to analyzing the singular configurations of redundant manipulators [8]. Luh and Gu [9] used the fact that a singularity occurs when $\det(\mathbf{J}\mathbf{J}^T) = 0$. However, this equation is particularly complex for a redundant manipulator with non-intersecting axes, as it involves a sum of trigonometric expressions in five joint angles, spans over two pages, and cannot be factored or simplified.

Indeed, the equation in question involves calculating the determinant of a 6×6 matrix whose components are complex trigonometric expressions. This equation is often impossible to analyze symbolically [5]. Therefore, other approaches have been expressed to find the singular configurations of these robot arms. Nokleby and Podhorodeski [10] developed a reciprocity-based approach based on the mutual reciprocity of the joint screws in the Canadarm2. In addition to identifying singular configurations, this approach can reveal the lost motion information by giving a screw that is reciprocal to all joint screws.

Orientation and position singularity analysis can be done separately based on the Jacobian partitioning and generating a zero block using the elementary transformation matrices [11,12]. However, this approach is only applicable to architectures with decoupled kinematics. Another method is to look at the 6-joint sub-groups of the Jacobian. Based on this approach, singularity occurs when all of these sub-groups become singular, and their determinants become zero [13]. Kong and Gosselin [14] analyzed Canadarm2 using the dependent screw suppression approach. This approach can find the rank deficiency of one of these sub-Jacobians; then, additional conditions for being in a singular configuration must be satisfied. However, these methods can only be used for redundant manipulators with simple structures.

Screw dependency analysis is another method used to identify singular configurations of a manipulator. While we recently applied it to Kinova's Link 6, a 6-DOF manipulator [15], as far as we are aware, this technique has not yet been used for redundant manipulators. This approach can reveal the geometry behind kinematic singularities, showing that for a configuration to be considered singular in a redundant manipulator, it must simultaneously satisfy two distinct geometric conditions.

All these methods can reveal information about kinematic singularities. However, 7R arms also have an algorithmic singularity, depending on how the arm angle is defined [5]. An algorithmic singularity occurs when the arm angle, as defined, has no connection to the self-motion vector [16]. As a result, it becomes impossible to separate the control of the arm angle from the control of the end-effector motion. In YuMi, when programming Cartesian moves, the user must always specify the arm angle, in addition to the end-effector pose. Thus, to control the end-effector pose and the arm angle, it is important to conduct an analysis of both types of singularities [5].

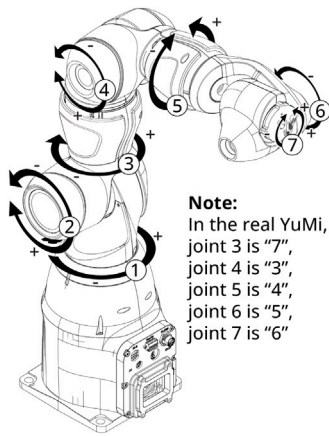
In order to comprehend the singularities of YuMi, we employ the screw dependency approach and evaluate their geometric conditions for categorization. According to this method, a kinematic singularity occurs when two separate linear dependencies exist between specific groups of joint screws, causing the end-effector to lose one of its motion capabilities.

In addition, we clearly define the arm angle in YuMi, which happens to be the same as in [5]. During a Cartesian move between two so-called robtargets with the same arm angle, the latter normally remains unchanged and is not automatically adjusted by some redundancy resolution algorithm. Therefore, it is up to the user to decompose the Cartesian move and specify the arm angle at each intermediate robtarget in order to avoid obstacles or singularities.

The remainder of this paper is organized as follows. In Section 2, the direct kinematic model of the single-arm YuMi is presented. In Section 3, the kinematic singularities of YuMi are categorized into different families in terms of their geometric conditions. In Section 4, the arm angle definition is given, and the algorithmic singularities are investigated. Section 5 discussed what YuMi's controller considers as singularities. Then Section 6 compares YuMi with a popular 7-DOF robot arm in terms of singularities. Finally, Section 7 concludes the paper and presents a summary of what is left for further investigation.

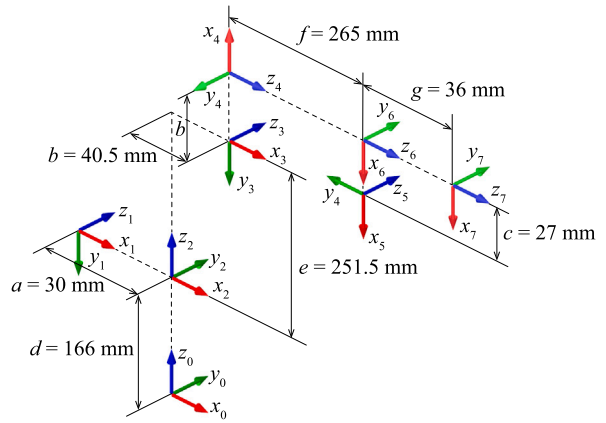
2. Single-arm YuMi model and its direct kinematics

The single-arm YuMi is a redundant manipulator with seven revolute joints, where every two consecutive joint axes are skew and normal to each other. Fig. 1 shows a schematic of the arm with its principal dimensions. To avoid confusion, we will use here the more common consecutive joint numbering; beware that the actual YuMi uses a different convention.



Note:
In the real YuMi,
joint 3 is "7",
joint 4 is "3",
joint 5 is "4",
joint 6 is "5",
joint 7 is "6"

(a) Joint directions and redefined joint numbering



(b) DH frames and parameters used (distances not to scale)

Fig. 1. The single-arm YuMi with all joints at zero degrees.

Table 1
DH parameters of YuMi.

i	θ_i	d_i	a_i	α_i
1	θ_1	d	$-a$	-90°
2	θ_2	0	a	90°
3	θ_3	e	b	-90°
4	$\theta_4 - 90^\circ$	0	b	-90°
5	$\theta_5 + 180^\circ$	f	c	-90°
6	θ_6	0	$-c$	90°
7	θ_7	g	0	0°

The Denavit and Hartenberg (DH) parameters and frames [17] of ABB's YuMi are given in Table 1 and Fig. 1(b). The DH parameters can be used to transform two consecutive frames into each other as:

$${}^{i-1}\mathbf{T} = \mathbf{T}_{z_{i-1}}(d_i)\mathbf{R}_{z_{i-1}}(\theta_i)\mathbf{T}_{x_i}(a_i)\mathbf{R}_{x_i}(\alpha_i). \quad (1)$$

Eq. (1) describes the position and orientation of frame F_i with respect to frame F_{i-1} , where $\mathbf{R}_{z_{i-1}}(\theta_i)$ represents a pure rotation about the z_{i-1} axis by θ_i , $\mathbf{T}_{z_{i-1}}(d_i)$ a pure translation along the z_{i-1} axis by b_i , $\mathbf{T}_{x_i}(a_i)$ a pure translation along the x_i axis by a_i , and $\mathbf{R}_{x_i}(\alpha_i)$ a pure rotation about the x_i axis by α_i [10], and the DH frames F_i are shown in Fig. 1(b). Therefore, two consecutive link-frames of a manipulator can be expressed with respect to each other using this homogeneous transformation matrix according to the manipulator's configuration. The direct kinematic equation can be obtained as:

$${}^0\mathbf{T} = {}^0\mathbf{T}_1\mathbf{T}_2\mathbf{T}_3\mathbf{T}_4\mathbf{T}_5\mathbf{T}_6\mathbf{T}_7, \quad (2)$$

where

$${}^{i-1}\mathbf{T} = \begin{bmatrix} \cos \theta_i & -\sin \theta_i \cos \alpha_i & \sin \theta_i \sin \alpha_i & a_i \cos \theta_i \\ \sin \theta_i & \cos \theta_i \cos \alpha_i & -\cos \theta_i \sin \alpha_i & a_i \sin \theta_i \\ 0 & \sin \alpha_i & \cos \alpha_i & d_i \\ 0 & 0 & 0 & 1 \end{bmatrix}. \quad (3)$$

By choosing an appropriate reference frame to represent joint screws, the Jacobian matrix can be made simpler [18,19]. Thus, the joint screws and the Jacobian can be determined by (4)–(13) when F_4 serves as the main reference frame of the i th joint. Thus, the joint screw ${}^4\mathcal{S}_i$ is expressed in the reference frame F_4 , and represents the infinitesimal motion of that joint:








$${}^4\mathcal{S}_i = \begin{bmatrix} {}^4\mathbf{e}_i \\ {}^4\mathbf{e}_i \times {}^4\mathbf{r}_i \end{bmatrix}, \quad (4)$$

where ${}^4\mathbf{e}_i$ is the unit vector along joint axis i , and ${}^4\mathbf{r}_i$ is the vector between the origins frames F_i and F_4 , both vectors expressed with respect to frame F_4 . We utilize Eqs. (1) to (4) to express these vectors in frame F_4 . We thus have

$${}^4\mathbf{J} = [{}^4\mathcal{S}_1 \quad {}^4\mathcal{S}_2 \quad {}^4\mathcal{S}_3 \quad {}^4\mathcal{S}_4 \quad {}^4\mathcal{S}_5 \quad {}^4\mathcal{S}_6 \quad {}^4\mathcal{S}_7], \quad (5)$$

Table 2

Kinematic singularities in YuMi. Category A: First condition is $\mathcal{L}_1 \equiv \mathcal{L}_3$. In each case, $\text{Rank}(\mathbf{J}) = 5$.

Case	Second condition	Examples of joint positions ^a
A_{1a}	$\mathcal{L}_3 \equiv \mathcal{L}_5$	$30^\circ, 0^\circ, 30^\circ, -90^\circ, 30^\circ, 30^\circ, 30^\circ$
A_{1b}	$\mathcal{L}_5 \equiv \mathcal{L}_7$	$30^\circ, 0^\circ, 30^\circ, 30^\circ, 30^\circ, 0^\circ, 30^\circ$
A_{1c}	$\mathcal{L}_2 \equiv \mathcal{L}_7$	$30^\circ, 0^\circ, 99.58^\circ, 69.34^\circ, -169.85^\circ, 69.66^\circ, 30^\circ$
A_{2a}	$\mathcal{L}_2, \mathcal{L}_4, \mathcal{L}_7$ are parallel and coplanar 	$30^\circ, 0^\circ, 0^\circ, -66.52^\circ, 90^\circ, 90^\circ, 30^\circ$
A_{2b}	$\mathcal{L}_2, \mathcal{L}_5, \mathcal{L}_7$ are concurrent and coplanar 	$30^\circ, 0^\circ, 100.28^\circ, 71.62^\circ, 10.92^\circ, 52.33^\circ, 30^\circ$
A_{3a}	$\mathcal{L}_2, \mathcal{L}_3, \mathcal{L}_5, \mathcal{L}_6$ belong to two planar pencils with a common line 	$30^\circ, 0^\circ, 99.09^\circ, 34.29^\circ, -80.53^\circ, 30^\circ, 30^\circ$
A_{3b}	$\mathcal{L}_2, \mathcal{L}_3, \mathcal{L}_4, \mathcal{L}_7$ belong to a regulus of lines 	$30^\circ, 0^\circ, 88.97^\circ, 0^\circ, -173.11^\circ, 42.93^\circ, 30^\circ$
A_{3c}	$\mathcal{L}_2, \mathcal{L}_5, \mathcal{L}_6, \mathcal{L}_7$ belong to two planar pencils with a common line 	$30^\circ, 0^\circ, -103.87^\circ, 74.33^\circ, 0^\circ, 31.34^\circ, 30^\circ$
A_{4a}	$\mathcal{L}_2, \mathcal{L}_3, \mathcal{L}_4, \mathcal{L}_5, \mathcal{L}_6$ are concurrent with two skew lines 	$30^\circ, 0^\circ, 110.57^\circ, -107.81^\circ, 69.27^\circ, 30^\circ, 30^\circ$
A_{4b}	$\mathcal{L}_2, \mathcal{L}_3, \mathcal{L}_4, \mathcal{L}_6, \mathcal{L}_7$ are concurrent with two skew lines 	$30^\circ, 0^\circ, 106.07^\circ, -102.18^\circ, 0^\circ, 5.91^\circ, 30^\circ$

^a Each joint angle of $\pm 30^\circ$ can be replaced with an arbitrary value.

where ${}^4\mathbf{J}$ is the Jacobian matrix expressed in frame F_4 . The Jacobian matrix relates the joint velocities of a robotic manipulator to the end-effector velocities by the following equation:

$$\dot{\mathbf{q}} = \mathbf{J}(\mathbf{q})^{-1} \dot{\mathbf{x}} \tag{6}$$

where $\dot{\mathbf{q}}$ is the vector of joint velocities and $\dot{\mathbf{x}}$ is the vector of end-effector velocities. The columns of this matrix ($\mathcal{S}_1, \mathcal{S}_2, \dots$, and \mathcal{S}_7) are calculated as follows:

$${}^4\mathcal{S}_1 = [-S_2C_3, -C_2, S_2S_3, hS_3, bS_2S_3, hC_3 + bC_2]^T, \tag{7}$$

$${}^4\mathcal{S}_2 = [S_3, 0, C_3, eC_3, bC_3 + a, -eS_3]^T, \tag{8}$$

$${}^4\mathcal{S}_3 = [0, -1, 0, 0, 0, b]^T, \tag{9}$$

$${}^4\mathcal{S}_4 = [0, 0, 1, 0, 0, 0]^T, \tag{10}$$

$${}^4\mathcal{S}_5 = [C_4, S_4, 0, 0, 0, b]^T, \tag{11}$$

$${}^4\mathcal{S}_6 = \begin{bmatrix} S_4S_5 \\ -C_4S_5 \\ C_5 \\ (-bC_5 + c)C_4 + fS_4C_5 \\ (-bC_5 + c)S_4 - fC_4C_5 \\ -fS_5 \end{bmatrix}, \tag{12}$$

$${}^4\mathcal{S}_7 = \begin{bmatrix} -S_4C_5S_6 + C_4C_6 \\ C_4C_5S_6 + S_4C_6 \\ S_5S_6 \\ ((-cC_6 + fS_6 + c)S_4 - bC_4S_6) S_5 \\ -((-cC_6 + fS_6 + c)C_4 + bS_4S_6) S_5 \\ (-cC_6 + fS_6 + c)C_5 + bC_6 \end{bmatrix}, \tag{13}$$

where $S_i = \sin \theta_i$, $C_i = \cos \theta_i$, and $h = a \cos \theta_2 + e \sin \theta_2 - a$.

3. Kinematic singularities

YuMi is in a kinematic singularity when the six rows of its Jacobian matrix are linearly dependent. In all other configurations, the arm can control its end-effector with all six DOFs, and in addition, the arm can possibly control some redundant self motion. That redundant motion will be studied in the next section. Here, we will employ the screw dependency approach and classify the different kinematic singularities based on simple geometric conditions [13,20].

The geometric conditions given here (Tables 2, 3, and Fig. 2) correspond to kinematic singularities, as proven by screw theory, but they are also associated with complex symbolic expressions resulting from the analysis of dependencies in the Jacobian matrix's

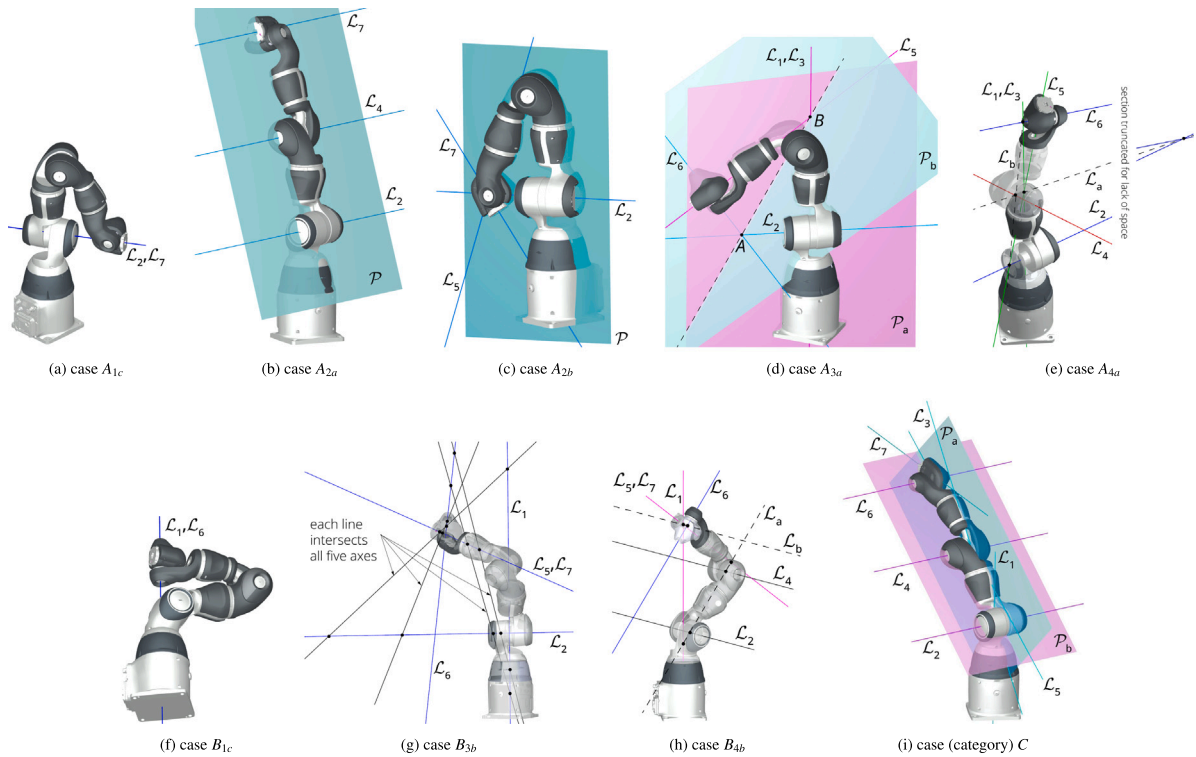


Fig. 2. Examples of YuMi's kinematic singularities.

Table 3
Kinematic singularities in YuMi. Category *B*: First condition is $\mathcal{L}_5 \equiv \mathcal{L}_7$. In each case, $\text{Rank}(\mathbf{J}) = 5$.

Case	Second condition	Examples of joint positions ^a
B_{1a}	$\mathcal{L}_3 \equiv \mathcal{L}_5$	$30^\circ, 30^\circ, 30^\circ, -90^\circ, 30^\circ, 0^\circ, 30^\circ$
B_{1b}	$\mathcal{L}_1 \equiv \mathcal{L}_3$	$30^\circ, 0^\circ, 30^\circ, 30^\circ, 30^\circ, 0^\circ, 30^\circ$
B_{1c}	$\mathcal{L}_1 \equiv \mathcal{L}_6$	$30^\circ, -79.96^\circ, 12.29^\circ, 79.73^\circ, -77.98^\circ, 0^\circ, 30^\circ$
B_{2a}	$\mathcal{L}_1, \mathcal{L}_4, \mathcal{L}_6$ are parallel and coplanar	$30^\circ, -90^\circ, 90^\circ, -78.98^\circ, 0^\circ, 0^\circ, 30^\circ$
B_{2b}	$\mathcal{L}_1, \mathcal{L}_3, \mathcal{L}_6$ are concurrent and coplanar	$30^\circ, -107.61^\circ, 9.57^\circ, 71.66^\circ, -80.98^\circ, 0^\circ, 30^\circ$
B_{3a}	$\mathcal{L}_2, \mathcal{L}_3, \mathcal{L}_5, \mathcal{L}_6$ belong to two planar pencils with a common line	$30^\circ, 30^\circ, 99.09^\circ, 34.29^\circ, -80.53^\circ, 0^\circ, 30^\circ$
B_{3b}	$\mathcal{L}_1, \mathcal{L}_2, \mathcal{L}_5, \mathcal{L}_6$ belong to a regulus of lines	$30^\circ, -34.93^\circ, 51.72^\circ, 0^\circ, -85.71^\circ, 0^\circ, 30^\circ$
B_{3c}	$\mathcal{L}_1, \mathcal{L}_4, \mathcal{L}_5, \mathcal{L}_6$ belong to a regulus of lines	$30^\circ, -45.25^\circ, 5.96^\circ, 0^\circ, -90.92^\circ, 0^\circ, 30^\circ$
B_{4a}	$\mathcal{L}_2, \mathcal{L}_3, \mathcal{L}_4, \mathcal{L}_5, \mathcal{L}_6$ are concurrent with two skew lines	$30^\circ, 30^\circ, 110.57^\circ, -107.81^\circ, 69.27^\circ, 0^\circ, 30^\circ$
B_{4b}	$\mathcal{L}_1, \mathcal{L}_2, \mathcal{L}_4, \mathcal{L}_5, \mathcal{L}_6$ are concurrent with two skew lines	$30^\circ, -52.74^\circ, 0^\circ, 15.68^\circ, 90^\circ, 0^\circ, 30^\circ$
B_{4c}	$\mathcal{L}_1, \mathcal{L}_3, \mathcal{L}_4, \mathcal{L}_5, \mathcal{L}_6$ are concurrent with two skew lines	$30^\circ, -14.22^\circ, 25.59^\circ, -85.94^\circ, 64.22^\circ, 0^\circ, 30^\circ$

^a Each joint angle of $\pm 30^\circ$ can be replaced with an arbitrary value.

columns. Indeed, we used these expressions to find numerical examples of kinematic-singularity joint sets that we present in this paper.

To identify a singular configuration in a redundant manipulator, we initially examine the relationships among the first six joint screws to identify linear dependencies [5,11]. To uncover the relationships among various combinations of joint screws, we conducted a comprehensive analysis. At the outset, we treat the seventh joint as the redundant joint. Next, we examine the interdependencies among the first six joint screws, using a novel combinatorial approach.

First, we focused on pairs of screws, examining dependencies such as $({}^4\mathcal{S}_1, {}^4\mathcal{S}_2)$, $({}^4\mathcal{S}_1, {}^4\mathcal{S}_3)$, all the way to $({}^4\mathcal{S}_5, {}^4\mathcal{S}_6)$. Next, we extended our analysis to three-screw dependencies, exploring combinations like $({}^4\mathcal{S}_1, {}^4\mathcal{S}_2, {}^4\mathcal{S}_3)$ and $({}^4\mathcal{S}_1, {}^4\mathcal{S}_2, {}^4\mathcal{S}_4)$. Finally, we delved into four-screw, five-screw, and six-screw dependencies, considering sets like $({}^4\mathcal{S}_1, {}^4\mathcal{S}_2, {}^4\mathcal{S}_3, {}^4\mathcal{S}_4)$, $({}^4\mathcal{S}_1, {}^4\mathcal{S}_2, {}^4\mathcal{S}_3, {}^4\mathcal{S}_4, {}^4\mathcal{S}_5)$, $({}^4\mathcal{S}_1, {}^4\mathcal{S}_2, {}^4\mathcal{S}_3, {}^4\mathcal{S}_4, {}^4\mathcal{S}_5, {}^4\mathcal{S}_6)$. To establish dependencies, we employed the concept of dependent vectors.

Here, we illustrate how we derived a dependency involving $({}^4\mathcal{S}_1, {}^4\mathcal{S}_6)$, and for the others, we utilized the same approach. To assess the dependency between these two screws, we arrange them into a 2×6 matrix. To determine their dependency, we repeatedly

remove four distinct rows and compute the determinant of the resulting 2×2 matrix, resulting in 15 different expressions. For these screws to be considered dependent, each of these 15 expressions must be zero. Consequently, we calculate these expressions and eliminate those that exhibit dependency or are already zero.

Up to this point, we identify all the dependencies among the first set of six joint screws. However, to be in a singular configuration, two different dependencies should be satisfied. Therefore, we need to apply, individually, each of these conditions for dependency to the Jacobian matrix to determine the dependencies among the second set of six joint screws (${}^4\mathcal{L}_2, {}^4\mathcal{L}_3, {}^4\mathcal{L}_4, {}^4\mathcal{L}_5, {}^4\mathcal{L}_6, {}^4\mathcal{L}_7$). To identify available dependencies among this set, we are using the same approach as for the first set of six joint screws.

Without this combinatorial approach, it is impossible to derive expressions for the cases of rank deficiency of the Jacobian matrix.

Finally, we categorize the exhaustive list of kinematic singularities, defined by symbolic expressions, based on different geometric conditions involving the joint axes, using Grassmann line geometry. We have two categories, depending on the first dependency condition, which is a simple one. Each of these categories is divided into sub-categories and cases. We also have a third category that has only one case.

3.1. Category A: $\mathcal{L}_1 \equiv \mathcal{L}_3$ (i.e., $\theta_2 = 0$)

In the first category, the first dependency is between the first and the third joint axes. This category can be further divided into three sub-categories, based on the number of joint axes involved in the second dependency, i.e., the second condition for singularity, as shown in Table 2. In each group of two, three, four or five joint axes, the sub-index, 1, 2, 3 or 4, respectively, corresponds to the number of linearly independent screws. In each case, the rank of the Jacobian drops to 5.

By defining \mathcal{L}_i as the i th joint axis, here are the four possible sub-categories for category A, each having several cases.

3.1.1. Sub-category A_1 : Two-screw dependencies

This sub-category covers three cases with one dependency between two joint screws:

A_{1a} : $\mathcal{L}_3 \equiv \mathcal{L}_5$ (shoulder–elbow singularity). This singularity occurs when axes 3 and 5 coincide too.

A_{1b} : $\mathcal{L}_5 \equiv \mathcal{L}_7$ (shoulder–wrist singularity). This singularity occurs when axes 5 and 7 coincide too.

A_{1c} : $\mathcal{L}_2 \equiv \mathcal{L}_7$. This singularity occurs when axes 2 and 7 coincide too (Fig. 2(a)).

3.1.2. Sub-category A_2 : Three-screw dependencies

This sub-category covers two cases with one dependency between three joint screws:

A_{2a} : $\mathcal{L}_2, \mathcal{L}_4,$ and \mathcal{L}_7 are parallel and coplanar. As shown in Fig. 2(b), $\mathcal{L}_2, \mathcal{L}_4,$ and \mathcal{L}_7 are parallel and lie in the same plane, \mathcal{P} .

A_{2b} : $\mathcal{L}_2, \mathcal{L}_5,$ and \mathcal{L}_7 are concurrent and coplanar. As shown in Fig. 2(c), $\mathcal{L}_2, \mathcal{L}_5,$ and \mathcal{L}_7 intersect each other at one point and lie in the same plane, \mathcal{P} .

3.1.3. Sub-category A_3 : Four-screw dependencies

This sub-category covers three cases with one dependency between four joint screws:

A_{3a} : $\mathcal{L}_2, \mathcal{L}_3, \mathcal{L}_5,$ and \mathcal{L}_6 are forming a union of two flat pencils having a common line, but lying in distinct planes and with distinct centers. As shown in Fig. 2(d), \mathcal{L}_2 and \mathcal{L}_6 intersect at point A and lie in plane \mathcal{P}_a , and \mathcal{L}_3 and \mathcal{L}_5 intersect at point B and lie in plane \mathcal{P}_b . Besides, planes \mathcal{P}_a and \mathcal{P}_b intersect at line AB .

A_{3b} : $\mathcal{L}_2, \mathcal{L}_3, \mathcal{L}_4,$ and \mathcal{L}_7 belong to a regulus of lines. This means that there are infinitely many lines that intersect $\mathcal{L}_2, \mathcal{L}_3, \mathcal{L}_4,$ and \mathcal{L}_7 . These lines belong to a hyperboloid of one sheet, forming a type of four-screw dependency [21]. This geometric condition is similar to the one demonstrated in Fig. 2(g).

A_{3c} : $\mathcal{L}_2, \mathcal{L}_5, \mathcal{L}_6,$ and \mathcal{L}_7 are forming a union of two flat pencils having a common line, but lying in distinct planes and with distinct centers. Specifically, \mathcal{L}_2 and \mathcal{L}_6 intersect at point A and lie in plane \mathcal{P}_a , and \mathcal{L}_5 and \mathcal{L}_7 intersect at point B and lie in plane \mathcal{P}_b . Besides, planes \mathcal{P}_a and \mathcal{P}_b intersect at line AB . Since this geometric condition is similar to that of case A_{3a} , we do not provide a figure.

3.1.4. Sub-category A_4 : Five-screw dependencies

This sub-category covers two cases with one dependency between five joint screws:

A_{4a} : $\mathcal{L}_2, \mathcal{L}_3, \mathcal{L}_4, \mathcal{L}_5,$ and \mathcal{L}_6 are concurrent with two skew lines. As shown in Fig. 2(e), \mathcal{L}_2 and \mathcal{L}_6 intersect at a point on a line \mathcal{L}_a , and \mathcal{L}_3 and \mathcal{L}_5 also intersect at a point on line \mathcal{L}_a . Similarly, \mathcal{L}_3 and \mathcal{L}_6 intersect at a point on a line \mathcal{L}_b , \mathcal{L}_2 and \mathcal{L}_5 also intersect at a point on line \mathcal{L}_b , and finally $\mathcal{L}_4, \mathcal{L}_a$ and \mathcal{L}_b intersect at one point. In other words, each of the five axes intersects both \mathcal{L}_a and \mathcal{L}_b .

A_{4b} : $\mathcal{L}_2, \mathcal{L}_3, \mathcal{L}_4, \mathcal{L}_6,$ and \mathcal{L}_7 are concurrent with two skew lines. Specifically, \mathcal{L}_3 and \mathcal{L}_7 intersect at one point, and there is a line \mathcal{L}_a passing through that point, intersecting \mathcal{L}_2 , and parallel to \mathcal{L}_4 and \mathcal{L}_6 . There is also a line \mathcal{L}_b that intersects all five joint axes. This case is similar to the previous one, so no figure is provided.

3.2. Category B: $\mathcal{L}_5 \equiv \mathcal{L}_7$ (i.e., $\theta_6 = 0$)

In the second category, the first dependency is between the fifth and the seventh joint axes. As with category A, category B can be divided into four sub-categories, based on the number of joint axes involved in the second dependency forming the second condition for singularity, as shown in Table 2. Again, the rank of the Jacobian drops to 5.

As in the case of category A, there are four possible sub-categories, each having several cases.

3.2.1. B_1 : Two-screw dependencies

This sub-category covers three cases with one dependency between two joint screws:

B_{1a} : $\mathcal{L}_3 \equiv \mathcal{L}_5$ (wrist–elbow singularity). This singularity occurs when axes 3 and 5 coincide too.

B_{1b} : $\mathcal{L}_1 \equiv \mathcal{L}_3$ (shoulder–wrist singularity). This case is identical to case A_{1b} .

B_{1c} : $\mathcal{L}_1 \equiv \mathcal{L}_6$. This singularity occurs when axes 1 and 6 coincide too, as shown in Fig. 2(f).

3.2.2. B_2 : Three-screw dependencies

This sub-category covers two cases with one dependency between three joint screws. The geometric conditions are simple, so no figures are provided.

B_{2a} : \mathcal{L}_1 , \mathcal{L}_4 , and \mathcal{L}_6 are parallel and coplanar.

B_{2b} : \mathcal{L}_1 , \mathcal{L}_3 , and \mathcal{L}_6 are concurrent and coplanar.

3.2.3. B_3 : Four-screw dependencies

This sub-category covers three cases with one dependency between four joint screws:

B_{3a} : \mathcal{L}_2 , \mathcal{L}_3 , \mathcal{L}_5 , and \mathcal{L}_6 are forming a union of two flat pencils having a common line, but lying in distinct planes and with distinct centers. This second condition is the same as the second condition of case A_{3a} .

B_{3b} : \mathcal{L}_1 , \mathcal{L}_2 , \mathcal{L}_5 , and \mathcal{L}_6 belong to a regulus of lines. In other words, as illustrated in Fig. 2(g), there are infinitely many lines that intersect \mathcal{L}_1 , \mathcal{L}_2 , \mathcal{L}_5 , and \mathcal{L}_6 .

B_{3c} : \mathcal{L}_1 , \mathcal{L}_4 , \mathcal{L}_5 , and \mathcal{L}_6 belong to a regulus of lines. In other words, there are infinitely many lines that intersect \mathcal{L}_1 , \mathcal{L}_4 , \mathcal{L}_5 , and \mathcal{L}_6 . This case is similar to the previous one.

3.2.4. B_4 : Five-screw dependencies

This sub-category covers three cases with one dependency between five joint screws:

B_{4a} : \mathcal{L}_2 , \mathcal{L}_3 , \mathcal{L}_4 , \mathcal{L}_5 , and \mathcal{L}_6 are concurrent with two skew lines. This second condition is identical to the second condition of case A_{4a} (Fig. 2(e)).

B_{4b} : \mathcal{L}_1 , \mathcal{L}_2 , \mathcal{L}_4 , \mathcal{L}_5 , and \mathcal{L}_6 are concurrent with two skew lines. Specifically, as shown in Fig. 2(h), there is a line \mathcal{L}_a that intersects \mathcal{L}_1 , \mathcal{L}_2 , \mathcal{L}_4 , and \mathcal{L}_5 , and is parallel to \mathcal{L}_6 (thus intersecting it at infinity). In addition, there is a \mathcal{L}_b that passes through the intersection point of \mathcal{L}_1 and \mathcal{L}_5 , intersects \mathcal{L}_6 , and is parallel to \mathcal{L}_2 and \mathcal{L}_4 , thus intersecting them at infinity.

B_{4c} : \mathcal{L}_1 , \mathcal{L}_3 , \mathcal{L}_4 , \mathcal{L}_5 , and \mathcal{L}_6 are concurrent with two skew lines. One of these two lines is parallel to \mathcal{L}_6 .

3.3. Category C

The last category is different as it does not involve two coincident axes. Also, it consists of a single case. Here, the two conditions are: three of the joint axes are coplanar and parallel, while the remaining four joint axes are coplanar [20]. Again, the rank of the Jacobian is 5, i.e., the robot end-effector loses one DOF. Specifically, we have

C: \mathcal{L}_2 , \mathcal{L}_4 , and \mathcal{L}_6 are parallel and coplanar, and \mathcal{L}_1 , \mathcal{L}_3 , \mathcal{L}_5 , and \mathcal{L}_7 are coplanar. An example of this singularity is shown in Fig. 2(i), where $\theta_3 = \theta_5 = 0$, and $\theta_4 = -71.42^\circ$.

3.4. Combinations

In all of these 21 cases of unique singularities, each composed of two different geometric conditions, there is only one end-effector DOF lost. However, some of these cases can be combined to lead to a loss of two end-effector DOFs. The pairs of conditions that can be combined are as follows: $\{A_{1a}, A_{1b}\}$ (i.e., $\mathcal{L}_1 \equiv \mathcal{L}_3 \equiv \mathcal{L}_5 \equiv \mathcal{L}_7$), $\{A_{1b}, A_{4a}\}$, and $\{A_{1b}, A_{3a}\}$. Other combinations of singularity cases can produce a singularity with two end-effector DOFs lost, but they do not create new singularities. For example, by combining B_{1b} and B_{4a} , we are generating the condition that is generated by combining A_{1b} and A_{4a} . Finally, in Category C, we can add the condition $\mathcal{L}_1 \equiv \mathcal{L}_7$ to produce a case with two end-effector DOFs lost.

It is impossible to lose three or more DOFs at the end-effector in YuMi. Indeed, it is easy to prove that joint screws ${}^4\mathcal{S}_2$, ${}^4\mathcal{S}_3$, ${}^4\mathcal{S}_4$, and ${}^4\mathcal{S}_5$, can never be linearly dependent.

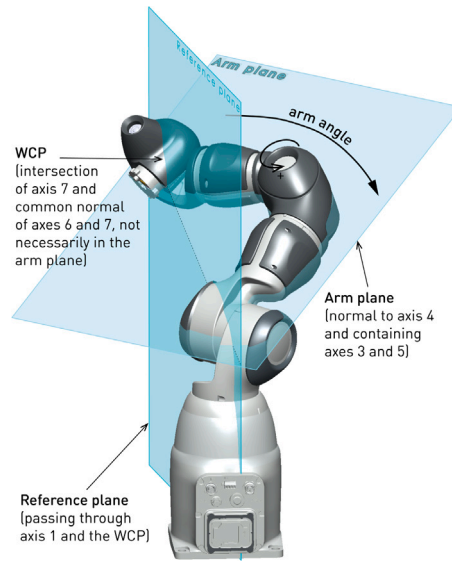


Fig. 3. Definition of the arm angle in YuMi.

4. Arm angle and algorithmic singularity

In YuMi, ABB defines the redundant self motion with an *arm angle* [22]. Whenever a user must specify a desired end-effector pose, they must also specify the arm angle. And while there is a command to automatically find the optimal so-called configuration of the robot (i.e., the solution of the inverse kinematics), there is no command to omit specifying an arm angle and let the robot automatically find an optimal one. Thus, users must know the exact definition of the arm angle, and we provide here a detailed explanation of this angle.

4.1. Definition of arm-angle and representation singularities

Loosely speaking, the arm angle defines the rotation of the elbow about an axis passing through some point in the shoulder and some other point in the wrist of the robot. Indeed, the desirable redundant self motion in YuMi is the swivel of joint axis 4, while the end-effector is fixed with respect to the base. Thus, when joint axes 3 and 5 are coincident, we still have the desirable self motion.

While the arm angle is easy to define in 7R arms where the first and last three axes are concurrent, YuMi's arm angle definition is more intricate. ABB defines the arm angle as the angle of the arm about a line passing through the “origin of axis 2” and the “wrist center point” (WCP), with no definition of the WCP [22]. Here, we present the exact definition of YuMi's arm angle, which happens to be the same as defined in [5]. While there are three different options for the so-called *reference direction* (axis 1, or the y or z axis of the world reference frame) that could be chosen in the controller parameters for the definition of the arm angle, we will consider joint axis 1 as the reference direction, since it is the most logical choice for a table-top installation, but the definition can be easily obtained for the other two options.

The arm angle is defined as the directed angle between two vectors that are normal to two planes, as shown in Fig. 3. The first plane, which we call the *reference plane*, is the plane containing axis 1 and the WCP. The so-called WCP was found to be the intersection point between axis 7 and the common normal to axes 6 and 7. The second plane is the *arm plane*, which has axis 4 as its normal vector and contains axes 3 and 5. Assuming that all vectors are expressed in the base reference frame, the arm angle ϕ is defined as:

$$\phi = \text{atan2}(\text{sign}(\mathbf{e}_3 \cdot \mathbf{e}_0) \|\mathbf{n} \times \mathbf{e}_3\|, \mathbf{n} \cdot \mathbf{e}_3), \quad (14)$$

where \mathbf{e}_3 is the unit vector along axis 4, or more precisely along z_3 (Fig. 1(b)), and \mathbf{n} is the unit vector normal to the plane containing axis 1 and the WCP, which we call the reference plane. Vector \mathbf{n} is calculated as follows:

$$\mathbf{n} = \frac{\mathbf{e}_0 \times \mathbf{w}}{\|\mathbf{e}_0 \times \mathbf{w}\|}, \quad (15)$$

where \mathbf{e}_0 is the unit vector along axis 1, defined by the right-hand rule, and \mathbf{w} is the position vector of the WCP.

When the WCP lies on axis 1, the above definition fails, leading to a *representation singularity*. In such configurations, YuMi's controller detects the singularity, preventing the robot from moving in Cartesian mode. To address this, ABB has implemented two alternatives for axis 1 in defining the reference plane [22]—the y or z axis of the world reference frame. By selecting an axis on which the WCP can never lie, representation singularities are avoided.

Table 4
Kinematically singular configurations of KUKA's iiwa.

Case	First condition	Second condition	Rank(J)
<i>A</i>	$\sin \theta_2 = 0$	$\cos \theta_3 = 0$	5
<i>B</i>	$\sin \theta_4 = 0$	–	5
<i>C</i>	$\cos \theta_5 = 0$	$\sin \theta_6 = 0$	5
<i>D</i>	$\sin \theta_2 = 0$	$\sin \theta_6 = 0$	5
<i>AB</i>	$\sin \theta_2 = 0, \cos \theta_3 = 0$	$\sin \theta_4 = 0$	4
<i>AD</i>	$\sin \theta_2 = 0, \cos \theta_3 = 0$	$\cos \theta_5 = 0, \sin \theta_6 = 0$	4
<i>BC</i>	$\sin \theta_4 = 0, \sin \theta_6 = 0$	$\sin \theta_4 = 0$	4
<i>ABCD</i>	$\sin \theta_2 = 0, \cos \theta_3 = 0, \sin \theta_4 = 0$	$\cos \theta_5 = 0, \sin \theta_6 = 0$	3

4.2. Algorithmic singularity

In an algorithmic singularity, there is a sudden change of the redundant self motion [5]. The arm-angle is still defined, but cannot be changed. In YuMi, there are two possibilities.

Shoulder algorithmic singularity

When $\theta_2 = 0$, the first and the third joint axes coincide and there is a self motion where joints 1 and 3 can rotate at the same speed in opposite directions. For all but two values of θ_3 , the arm-angle self motion is impossible.

Wrist algorithmic singularity

Similarly, when $\theta_6 = 0$, the fifth and the seventh joint axes coincide and there is a self motion where joints 5 and 7 can rotate at the same speed in opposite directions. For all but two values of θ_5 the arm-angle self motion is impossible.

Contrary to [5], which studied essentially the same manipulator as YuMi, we do not consider the configuration $\theta_4 = -90^\circ$ (i.e., when joint axes 3 and 5 coincide) as an algorithmic singularity because ABB's arm angle is well-defined. Indeed, the resulting self motion is exactly the default arm-angle motion, although we agree that in this configuration, the self motion is less useful. For example, the redundant DOF cannot be used to avoid obstacles, nor to move away from a singularity.

4.3. Avoidability of kinematic singularities

One of the advantages of 7-DOF arms is that we can use the self motion in order to avoid a kinematic singularity for a given pose. As we saw in Section 3, all but two cases of Category *A* kinematic singularities depend on axis 2. Therefore, by simply rotating the self motion about the coinciding axes 1 and 3, we can escape the kinematic singularity, while keeping the pose of the end-effector. Similarly, all but two cases of Category *B* kinematic singularities depend on axis 6. Therefore, by simply rotating the self motion about the coinciding axes 5 and 7, we can escape the kinematic singularity, while keeping the pose of the end-effector. Grant et al, in ABB, none of these two self motions can be controlled by the user in Cartesian mode, since they are not associated with the arm angle. However, if one needs the end-effector to be at a pose that corresponds to one of these kinematic singularities, it is possible to calculate (though not in ABB's software) a joint position for which there is no kinematic singularity.

As for Category *C*, it is generally possible to rotate the arm angle, as defined by ABB, and exit the kinematic singularity (though this cannot be done in ABB's software).

Therefore, the only end-effector poses that cannot be reached in a joint position that does not correspond to a kinematic singularity is those for which we have any two of the following three conditions: $\theta_2 = 0$, $\theta_4 = -90^\circ$ and $\theta_6 = 0$.

5. Singularities of YuMi according to ABB

According to the technical documentation of ABB [22], serial link robots with seven axes, such as the IRB 14000/14050, have all the singularities of 6-axis robots but also have two additional singularities. The first of these is when joint 2 has an angle equal to zero so that joint axes 1 and 3 become coincident. This is similar to the wrist singularity. The second singularity is related to the calculation of the arm angle and varies depending on which reference direction is configured since the singularity occurs when the WCP is in the reference direction.

In reality, YuMi's robot controller seems to be programmed to consider the following three configurations as problematic, in addition to the representation singularity:

- $\theta_2 = 0$, i.e., when joint axes 1 and 3 coincide;
- $\theta_6 = 0$, i.e., when joint axes 5 and 7 coincide;
- loosely speaking, when the arm is “fully stretched” as in Fig. 4, and the 6×6 Jacobian matrix of a robot obtained by removing the redundant joint 3 from YuMi is singular.

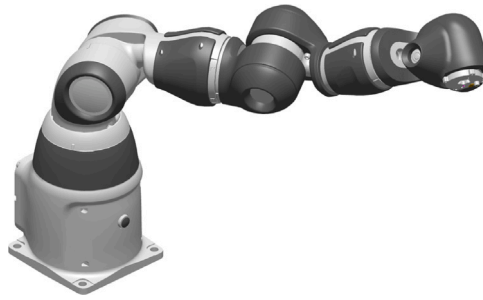


Fig. 4. Example of a “kinematic limitation” according to ABB, for the joint position $\{30^\circ, -89.48^\circ, 17.32^\circ, -62.73^\circ, 122^\circ, 80.72^\circ, 30^\circ\}$.

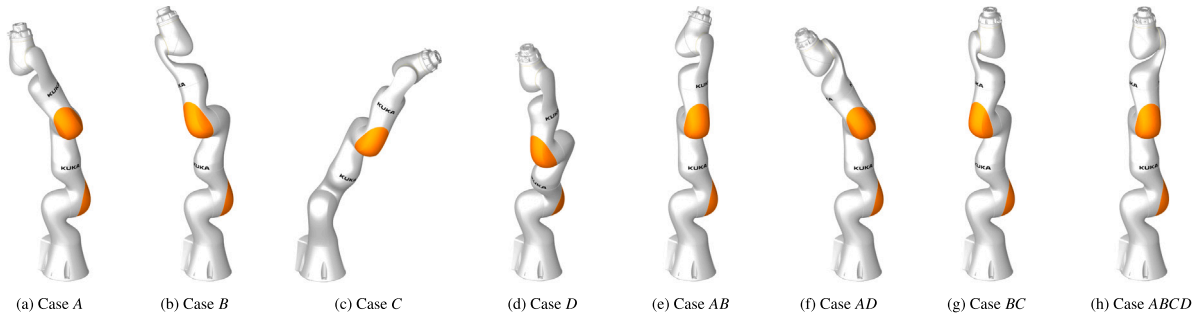


Fig. 5. The kinematic singularities of KUKA’s iiwa 7-DOF robot arm. Note that all unimportant angles were assigned the value of 30° or -30° , as we did in Fig. 2, which is why all configurations seem similar.

The third configuration is actually reported by the controller as a “kinematic limitation”. In that configuration, YuMi’s controller cannot rotate the arm angle in one direction, even though the physical arm-angle self motion is not restrained.

The combination of these three boundary conditions is used to designate the maximum of eight configurations that ABB’s RobotStudio software proposes as different solutions to the inverse kinematics of YuMi, for a given arm angle, in the same fashion as the well-known {front/back, elbow-up/elbow-down, flip/noflip} configuration parameters of traditional, PUMA-like 6-DOF robot arms.

While these three configurations are not kinematic singularities, ABB is right to consider the first two, which are algorithmic singularities, as problematic since, as already mentioned, users must always specify the arm angle for Cartesian moves, rather than let the robot use some redundancy-resolution technique. As for the third configuration, while it represents no singularity at all, it is close to a workspace limit.

As summarized in Tables 2 and 3, we showed that all but one of the actual kinematic singularities in YuMi require that $\theta_2 = 0$ (category A) or $\theta_6 = 0$ (Category B). Thus, ABB has simplified its approach to managing kinematic singularities, by considering only the first of the two conditions for a kinematic singularity of categories A and B.

We must also add that YuMi’s controller does detect the kinematic singularities of category C (Fig. 2(i)) as problematic and reports them as “kinematic limitations”. This is simply because the numerical method used fails to find an inverse kinematic solution. However, it also reports as problematic configurations like the one in Fig. 4, that are close to but not singular.

6. Comparison between KUKA’s iiwa and YuMi

To conclude, we compare YuMi’s singularities to those of a 7R robot arm with zero offsets, like KUKA’s LBR iiwa. A description of iiwa’s singularities has been given in [16], for example. In our comparison, we evaluate the singularities of these two redundant arms in terms of the rank of the Jacobian matrix, the number of lost end-effector DOFs, and the avoidability of the singularities. The singular conditions for KUKA’s iiwa are summarized in Fig. 5 and Table 4. Not only does iiwa have fewer kinematic singularities, but they are simpler to describe.

6.1. Number of lost end-effector DOFs

As we saw, in YuMi, the rank of the Jacobian is always greater than four, which means that YuMi’s end-effector loses at most two DOFs when in a kinematic singularity. However, KUKA’s iiwa can lose one, two, or three DOFs [16]. For example, iiwa’s end-effector loses three DOFs when all of the different kinematic singularity conditions occur (case ABCD, Table 4).

6.2. Avoidability of kinematic singularities

There is little difference between YuMi and iiwa in their ability to escape kinematic singularities through the use of the available self motion. In iiwa too, to escape the most frequent kinematic singularities (cases *A* and *C*), the redundant self motion to use is not the arm angle.

7. Conclusion and further work

In this paper, we demonstrated that the kinematic singularities of YuMi are completely different from the well-known wrist, elbow, and shoulder singularities of typical 6-DOF, PUMA-type robots. We also showed that YuMi has a greater variety of singularities compared to a 7-DOF robot arm without joint offsets.

Specifically, we presented for the first time simple geometric conditions for each kinematic singularity, giving a more precise understanding of the robot's kinematics. Furthermore, we showed that in some specific singular configurations, YuMi's end-effector loses two degrees of freedom, but it can never lose three DOFs, unlike other 6- and 7-DOF robot arms.

It should be noted that the authors of [5], who studied a manipulator identical to YuMi, did not find the robot's kinematic singularities. Instead, they derived the kinematic singularities of a simplified version of the manipulator, where one of the joint offsets was set to zero.

Moreover, ABB's definition of the arm angle was given as the angle between the arm plane normal to joint axis 4 and the reference plane that runs through axis 1 and a special point WCP on joint axis 7. Although this was already done in [5], for completeness, we also provided the representation singularity where this particular arm-angle definition fails. Similarly, the two algorithmic singularities were discussed: the shoulder algorithmic singularity, and the wrist algorithmic singularity. In each of these two configurations, the arm-angle self motion is generally lost and the redundant DOF becomes different.

By identifying and categorizing the various singular configurations, this paper equips researchers and engineers with essential information to develop more efficient and robust robot control strategies. Understanding the conditions under which the robot is in a singularity allows for better motion planning. The insights gained from this study are invaluable for optimizing YuMi's performance, ensuring safe and efficient robot operation, and enhancing its usability in diverse real-world scenarios. The study can also be applied to other 7-DOF robot arms with complex kinematics, such as those from Kassow Robots, for which no geometric description is yet available.

The inverse kinematics of YuMi remains a challenge and no analytical solution is currently available. As a result, in future works, we will attempt to derive an analytic solution for the robot's inverse kinematic problem. Besides, we intend to propose an algorithm to automatically manage the self motion in YuMi and avoid kinematic singularities. Furthermore, we intend to work on a better way of proposing a set of inverse kinematic solutions for a given end-effector pose.

Finally, our novel approach to analyzing the singularities of a 7-DOF robot arm can be applied to other similar designs, such as the very similar one studied in [5], or the collaborative robots of Kassow Robots.

CRedit authorship contribution statement

Milad Asgari: Writing – original draft, Validation, Methodology, Investigation, Formal analysis, Conceptualization. **Ilian A. Bonev:** Writing – review & editing, Visualization, Validation, Supervision, Conceptualization. **Clément Gosselin:** Writing – review & editing, Supervision, Funding acquisition.

Declaration of competing interest

The authors declare the following financial interests/personal relationships which may be considered as potential competing interests: Milad Asgari reports financial support was provided by Quebec Research Fund Nature and Technology. If there are other authors, they declare that they have no known competing financial interests or personal relationships that could have appeared to influence the work reported in this paper.

Acknowledgments

This work was funded by the Fonds de Recherche du Québec, Nature et Technologie (FQRNT).

Data availability

No data was used for the research described in the article.

References

- [1] I. Kuhlemann, P. Jauer, F. Ernst, A. Schweikard, Robots with seven degrees of freedom: Is the additional DoF worth it? in: 2nd International Conference on Control, Automation and Robotics, ICCAR, 2016.
- [2] M. Slim, N. Rokbani, B. Neji, M.A. Terres, T. Beyrouthy, Inverse kinematic solver based on bat algorithm for robotic arm path planning, *Robotics* 12 (2) (2023) 38.
- [3] R. Ravindran, K. Doetsch, Design aspects of the shuttle remote manipulator control, in: Guidance and Control Conference 1982 Aug 17, 1982, p. 1581.
- [4] D. Pieper, *The Kinematics of Manipulators under Computer Control*, Stanford University, 1969.
- [5] K. Kreutz-Delgado, M. Long, H. Seraji, Kinematic analysis of 7-DOF manipulators, *Int. J. Robot. Res.* 11 (5) (1992) 469–481.
- [6] A. Almarkhi, A. Maciejewski, Singularity analysis for redundant manipulators of arbitrary kinematic structure, in: *Proceeding of the 16th International Conference on Informatics in Control, Automation and Robotics*, 2019, <http://dx.doi.org/10.5220/0007833100420049>.
- [7] K.H. Hunt, Robot kinematics—A compact analytic inverse solution for velocities, *J. Mech. Transm. Autom. Des.* 109 (1) (1987) 42–49.
- [8] D. Whitney, Resolved motion rate control of manipulators and human prostheses, *IEEE Trans. Man Mach. Syst.* 10 (2) (1969) 47–53.
- [9] J. Luh, Y. Gu, Industrial robots with seven joints, in: *Proceedings of the IEEE International Conference on Robotics and Automation*, 1985.
- [10] S.B. Nokleby, R.P. Podhorodeski, Velocity degeneracy determination for the kinematically redundant CSA/ISE STEAR testbed manipulator, *J. Robot. Syst.* 17 (2000) 633–642.
- [11] G. Chen, L. Zhang, Q. Jia, H. Sun, Singularity analysis of the redundant robot with the structure of three consecutive parallel axes, *Found. Appl. Intell. Syst.* 77 (2013) 9–791.
- [12] W. Xu, J. Zhang, H. Qian, Y. Chen, Y. Xu, Identifying the singularity conditions of Canadarm2 based on elementary Jacobian transformation, in: *Proceedings of the IEEE/RSJ International Conference on Intelligent Robots and Systems*, 2013.
- [13] C.D. Crane III, J. Duffy, T. Carnahan, A kinematic analysis of the space station remote manipulator system (SSRMS), *J. Robot. Syst.* 8 (1991) 637–658, <http://dx.doi.org/10.1002/rob.4620080505>.
- [14] X. Kong, C.M. Gosselin, A dependent-screw suppression approach to the singularity analysis of a 7-DOF redundant manipulator: CANADARM2, *Trans. Can. Soc. Mech. Eng.* 29 (2005) 593–604, <http://dx.doi.org/10.1139/tcsme-2005-0038>.
- [15] M. Asgari, I.A. Bonev, C.M. Gosselin, Singularity analysis of Kinova's link 6 robot arm via Grassmann line geometry, in: *Proceedings of the IEEE International Conference on Robotics and Automation*, 2004.
- [16] L. Zhang, S. Guo, Y. Huang, X. Xiong, Kinematic singularity analysis and simulation for 7DOF anthropomorphic manipulator, *Int. J. Mechatron. Appl. Mech.* 6 (2019).
- [17] J. Denavit, R.S. Hartenberg, A kinematic notation for lower-pair mechanisms based on matrices, *J. Appl. Mech.* 22 (1955) 215–221, <http://dx.doi.org/10.1115/1.4011045>.
- [18] K.J. Waldron, S.-L. Wang, S.J. Bolin, A study of the Jacobian matrix of serial manipulators, *J. Mech. Transm. Autom. Des.* 107 (1985) 230–237, <http://dx.doi.org/10.1115/1.3258714>.
- [19] W. Khalil, É. Dombre, *Modeling, Identification and Control of Robots*, Hermes Penton, 2004.
- [20] Z. Huang, Q. Li, H. Ding, Dependency and reciprocity of screws, *Theory Parallel Mech.* (2012) 17–45, http://dx.doi.org/10.1007/978-94-007-4201-7_2.
- [21] T. Mbarek, G. Lonij, B. Corves, Singularity analysis of a fully parallel manipulator with five-degrees-of-freedom based on Grassmann line geometry, in: *Proceedings of the 12th IFToMM World Congress*, 2007.
- [22] ABB, *Technical reference manual, RAPID overview*, 2022.